ARTICLE   **Open Access**

Ultralow-field magnetocaloric materials for compact magnetic refrigeration

Peng Liu[1,2], Dongsheng Yuan [3], Chao Dong[4], Gaoting Lin [5], Encarnación G. Víllora[3], Ji Qi[1,2], Xinguo Zhao[1,2], Kiyoshi Shimamura[3], Jie Ma [2,4,5], Junfeng Wang [4], Zhidong Zhang [1,2] and Bing Li [1,2]

Abstract
Magnetic refrigeration around the liquid-helium temperature plays a critical role in many technological sectors. Even if gallium gadolinium garnet (GGG) has been regarded as the benchmark, its application is highly limited by the small magnetic entropy changes, the requirement of superconducting magnets, and the large device sizes. Here, we report that LiREF$_4$ (RE = rare earth) single crystals exhibit significantly superior magnetocaloric performance levels to commercial GGG. Under a small magnetic field of 5 kOe, which can be easily achieved by a permanent magnet, the magnetic entropy change reaches a record-high value of 16.7 J kg^{-1} K^{-1} in LiHoF$_4$ in contrast to the value of 1.0 J kg^{-1} K^{-1} in GGG. The combination of small driving fields, large entropy changes, and excellent thermal and/or magnetic reversibility enables this series to be employed as the ideal working material for compact magnetic refrigeration around the liquid-helium temperature.

Introduction

The magnetocaloric effect (MCE) is known as the thermal response of a magnetic material to changes in external magnetic fields. In the vicinity of a magnetic phase transition, external magnetic fields can effectively tune the entropy of the magnetic sublattice. When the magnetized material is demagnetized, a temperature drop is obtained. Such an effect was observed more than one hundred years ago. In 1926, Debye and Giauque theoretically deduced the possibility of adiabatic demagnetization refrigeration based on the MCE[1]. Subsequently, Giauque and MacDougall first used Gd$_2$(SO$_4$)$_3$·8H$_2$O as a magnetic coolant in adiabatic demagnetization refrigeration technology to achieve ultralow temperatures down to 0.25 K[2]. Since then, magnetic refrigeration technology based on the

MCE has received extensive attention, and thus far, it has been widely used in many fields, such as cooling bolometers for astrophysical measurements in space, providing a cryogenic environment for quantum computing and the production of superfluid liquid helium[3–12]. Due to the solid nature of the working materials, in particular, it is more appealing for space applications without the influences of gravity over fluid-based technology options such as ^{3}He/^{4}He dilution refrigeration.

The critical issue of the development of magnetic refrigeration technology is the identification of more efficient magnetocaloric materials with a larger isothermal magnetic entropy change (ΔS_m), larger adiabatic temperature change (ΔT_{ad}), and smaller driving magnetic field (ΔH). Therefore, extensive efforts have been devoted to tackling this challenge. In 1973, Fisher et al. systematically studied the thermomagnetic properties of gallium gadolinium garnet (GGG) single crystals along the [001], [110], and [111] directions, and the maximum ΔS_m reached 38 J kg^{-1} K^{-1} under a magnetic field change of 70 kOe[13–15]. Since then, GGG has become the primary choice for commercial adiabatic demagnetization refrigerators around the liquid-helium temperature as well as a

Correspondence: Dongsheng Yuan (YUAN.Dongsheng@nims.go.jp) or Junfeng Wang (jfwang@hust.edu.cn) or Bing Li (bingli@imr.ac.cn)
^{1}School of Materials Science and Engineering, University of Science and Technology of China, 72 Wenhua Road, 110016 Shenyang, Liaoning, China
^{2}Shenyang National Laboratory for Materials Science, Institute of Metal Research, Chinese Academy of Sciences, 72 Wenhua Road, 110016 Shenyang, Liaoning, China
Full list of author information is available at the end of the article
These authors contributed equally: Peng Liu, Dongsheng Yuan.

benchmark for magnetocaloric materials exploration[16,17]. Although an increasing number of low-temperature magnetocaloric materials with large ΔS_m values have been reported[18–22] to satisfy the growing demands for space exploration and quantum computation, strong magnetic fields are usually needed, which are currently only provided by heavy and large superconducting magnets. Furthermore, as commercial adiabatic demagnetization refrigerators are usually applied for precision detection in low-temperature environments, magnetic shielding must be considered. Both of the above aspects increase the cost and complicate the design of refrigeration systems. In addition, the low volume ratio of the magnetocaloric material to the magnetic refrigeration device results in bulky systems. These disadvantages have hindered practical application of magnetic refrigeration technology. Therefore, a material possessing excellent magnetocaloric performance under a magnetic field lower than 10 kOe provided by permanent magnets can significantly improve the efficiency of magnetic refrigeration equipment and facilitate the manufacture of more compact equipment.

Compounds consisting of rare earth (RE) elements usually exhibit excellent magnetocaloric properties due to their large intrinsic magnetic moments. Among them, lithium rare earth fluorides with the chemical formula $LiREF_4$ have a tetragonal scheelite structure (space group $I4_1/a$), where RE can comprise rare earth elements including gadolinium (Gd), terbium (Tb), dysprosium (Dy), holmium (Ho), erbium (Er), thulium (Tm), and ytterbium (Yb). The unit cell of $LiREF_4$ contains two magnetically equivalent trivalent lanthanide ions at sites with S_4 point symmetry. They exhibit exotic physical properties at low temperatures[23–34], such as quantum criticality. In regard to their basic magnetism, they can be categorized into three groups, namely, $LiTmF_4$, which is Van-Vleck paramagnetic[31]; $LiTbF_4$ and $LiHoF_4$, which are ferromagnetic (FM) with Curie temperature (T_C) values of 2.87 and 1.53 K, respectively[24–26,28,29]; and $LiDyF_4$, $LiErF_4$, and $LiYbF_4$, which are antiferromagnetic (AFM) with Néel temperature (T_N) values of 0.62, 0.38 and 0.128 K, respectively[27,30–32]. Currently, the magnetic ground state of $LiGdF_4$[23] is still unknown. $LiREF_4$ single crystals exhibit extremely high magnetocrystalline anisotropy due to crystal electric field effects[33]. The magnetic easy axes of $LiGdF_4$, $LiTbF_4$, and $LiHoF_4$ are parallel to the c axis, while those of $LiDyF_4$, $LiErF_4$, $LiYbF_4$, and $LiTmF_4$ are perpendicular to the c axis. The high magnetocrystalline anisotropy underlies the rotating MCEs, where MCE materials are rotated in the static magnetic fields between the easy and hard axes, corresponding to magnetization and demagnetization. A summary of the basic crystal structure and magnetism is shown in Fig. 1.
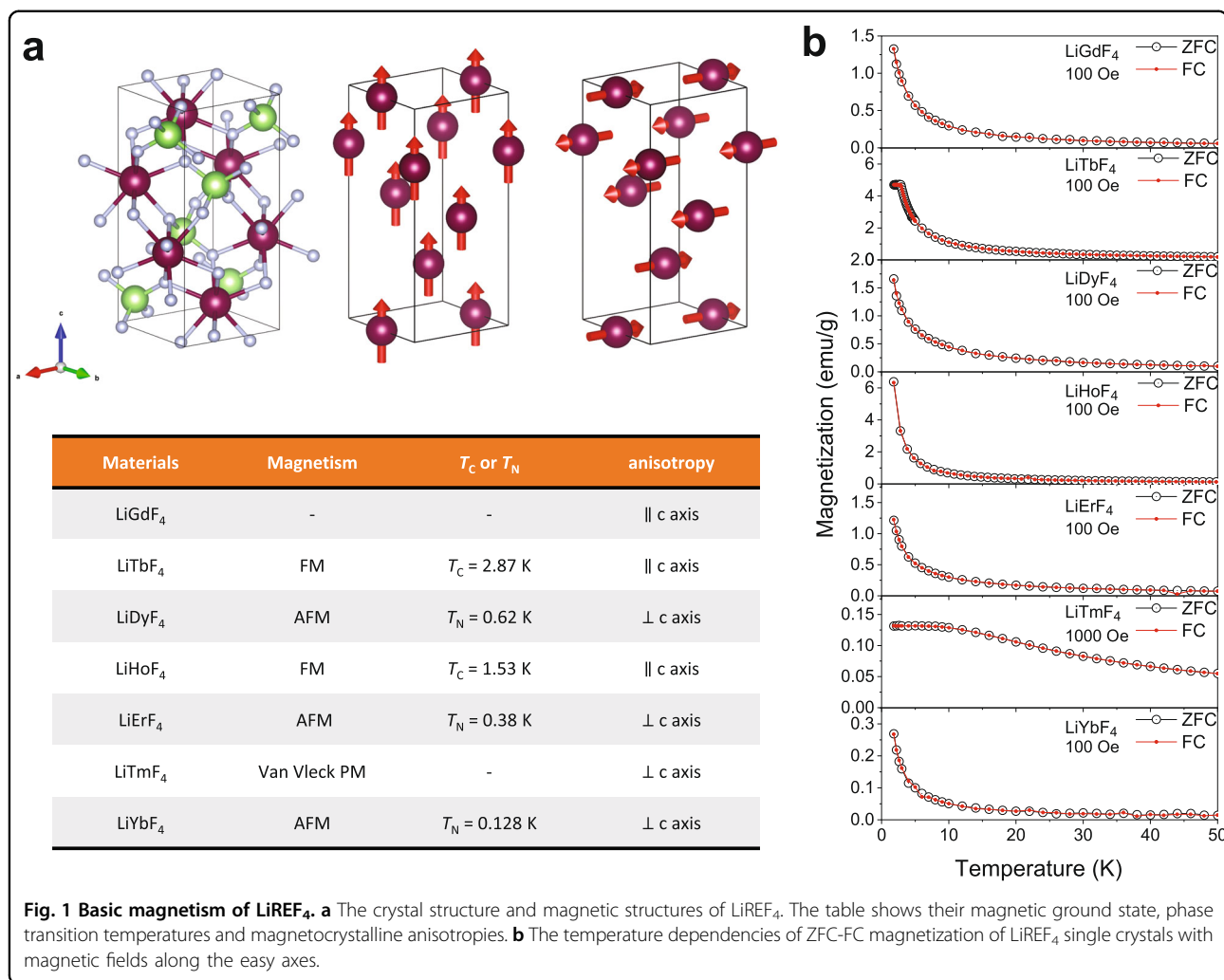
In this work, the magnetocaloric properties of $LiREF_4$ single crystals were systematically studied. These compounds exhibit extraordinary performance levels, much higher than that of the prototype GGG. Under a magnetic field as low as 5 kOe, the largest ΔS_m values was obtained in $LiHoF_4$, at approximately 16.7 J kg^{-1} K^{-1}. The largest entropy changes (ΔS_r) of rotating MCEs were also achieved in $LiHoF_4$, at approximately 16.5 J kg^{-1} K^{-1} under 5 kOe, 21.1 J kg^{-1} K^{-1} under 10 kOe and 22.6 J kg^{-1} K^{-1} under 20 kOe. More importantly, the direct ΔT_{ad} value of FM $LiHoF_4$ is approximately 2.38 K under 5 kOe using the pulsed magnetic field method. This remarkable performance renders $LiREF_4$ a promising next-generation working material for magnetic refrigerators around the liquid-helium temperature.

Results

Magnetic properties of $LiREF_4$ single crystals

Zero-field cooled (ZFC) and field-cooled (FC) magnetization curves were collected as a function of the temperature in the temperature range from 2 to 50 K for the above seven compounds. A magnetic field of 100 Oe was applied to the crystals along their magnetic easy axes except for $LiTmF_4$. Due to the weak magnetism of $LiTmF_4$, the applied magnetic field was 1000 Oe. $LiTbF_4$ experienced a FM transition at approximately 2.85 K, which is consistent with previous reports[24–26]. The magnetization for all compounds increased upon cooling, but no long-range magnetic order was found for the other fluorides above 1.8 K. Among these seven fluorides, $LiTmF_4$ exhibited a different tendency, and the ZFC and FC curves of $LiTmF_4$ showed that magnetization is a temperature-independent phenomenon below 8 K, which is a sign of Van-Vleck paramagnetism[31]. Notably, the ZFC and FC curves of all compounds overlapped, indicating high thermal reversibility.

Magnetic isotherms were measured in the temperature region from 1.8 to 24 K in very fine steps up to 20 kOe along both the easy and hard axes for the seven fluorides. The isothermal magnetization curves of $LiGdF_4$, $LiTbF_4$, and $LiHoF_4$ are shown in Supplementary Figs. 1–3, while those of $LiDyF_4$, $LiErF_4$, $LiYbF_4$ and $LiTmF_4$ are shown in Supplementary Figs. 4–7. Based on the single-crystal alignment (refer to the Methods section below) and magnetization curves, we determined that the magnetic easy axes of the former three fluorides are parallel to the c axis, whereas those of the latter four fluorides are perpendicular to the c axis. Their magnetocrystalline anisotropic properties are consistent with previously reported g-values of the system[33]. Along the easy axis, the magnetization of $LiTbF_4$ and $LiHoF_4$ at the lowest temperature increased so rapidly with increasing magnetic field that they were almost saturated at approximately 10 kOe. This feature suggests that they are FM in nature. The
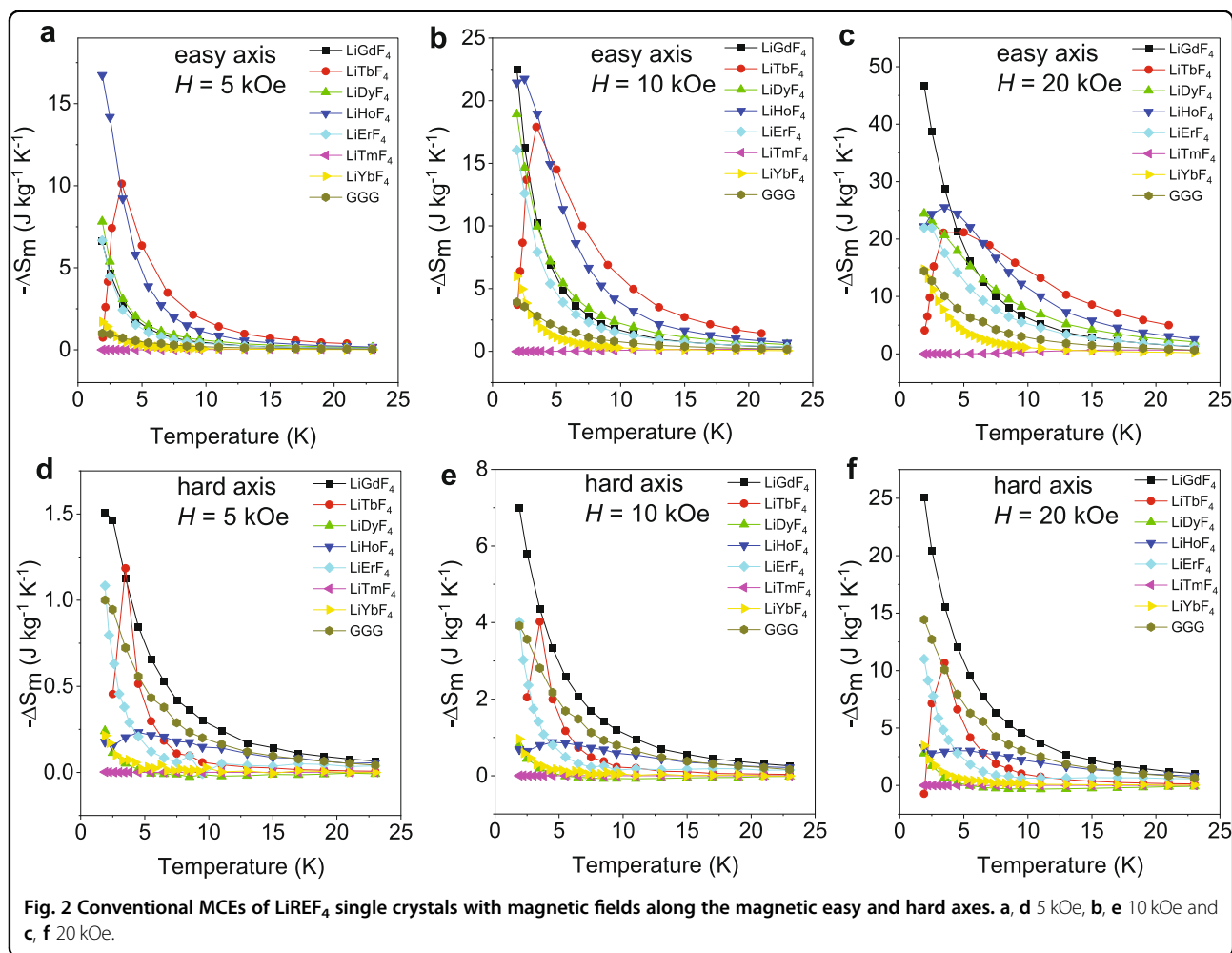
Fig. 1 Basic magnetism of LiREF₄. a The crystal structure and magnetic structures of LiREF₄. The table shows their magnetic ground state, phase transition temperatures and magnetocrystalline anisotropies. **b** The temperature dependencies of ZFC-FC magnetization of LiREF₄ single crystals with magnetic fields along the easy axes.

saturation magnetization approached 8.7 and 7.2 μ_B/RE^{3+} for $LiTbF_4$ and $LiHoF_4$, respectively. In this temperature region, $LiGdF_4$, $LiDyF_4$ and $LiErF_4$ exhibit PM properties, but with notable magnetic fluctuations so that the magnetization also rapidly increased under low fields. This is similar to PM $LiYbF_4$. However, the magnetic isotherms of $LiTmF_4$ were almost linear, which is consistent with the nature of Van-Vleck paramagnetism.

It is clear that the magnetization along the easy axes is much higher than that along the hard axes under small fields, indicating the high magnetocrystalline anisotropy of $LiREF_4$. $LiDyF_4$ exhibited the largest difference. At 1.8 K, the magnetization reached approximately 6.9 μ_B/RE^{3+} along the easy axis and below 0.84 μ_B/RE^{3+} along the hard axis, which suggests a remarkable rotating MCE. In addition, the magnetization along the hard axis did not decrease continuously with increasing temperature. Supplementary Fig. 8 shows $M-T$ curves under increasing magnetic fields. With decreasing temperature, the magnetization of the $LiDyF_4$ single-crystal sample first

increased, then decreased, and finally increased again due to the crystal electric field effects[27].

Conventional MCEs of LiREF₄

The temperature dependency of the isothermal entropy change ΔS_m for $LiREF_4$ under magnetic field variations of 5, 10, and 20 kOe along the easy and hard axes is shown in Fig. 2, where the data for the GGG single crystal are also included for comparison. Along the easy axes, the maxima of $-\Delta S_m$ for $LiGdF_4$, $LiTbF_4$, $LiHoF_4$, $LiDyF_4$, $LiErF_4$, $LiYbF_4$, and $LiTmF_4$ single crystals were 6.6, 10.1, 16.7, 7.8, 6.7, 1.7, and 0.04 J kg^{-1} K^{-1}, respectively, when the magnetic field was changed from 0 to 5 kOe, 22.5, 17.9, 21.7, 18.9, 16.1, 6, and 0.16 J kg^{-1} K^{-1}, respectively, when the magnetic field was changed from 0 to 10 kOe, and 46.7, 21.2, 25.5, 24.4, 21.9, 14.7, and 0.7 J kg^{-1} K^{-1}, respectively, when the magnetic field was changed from 0 to 20 kOe. Under a magnetic field of 5 kOe, $LiHoF_4$ yielded the largest $-\Delta S_m$ value among all fluorides, larger than that of polycrystalline $LiHoF_4$[21]. With increasing magnetic

Fig. 2 Conventional MCEs of LiREF$_4$ single crystals with magnetic fields along the magnetic easy and hard axes. a, **d** 5 kOe, **b**, **e** 10 kOe and **c**, **f** 20 kOe.

field, LiGdF$_4$ performed the best under 10 and 20 kOe. The corresponding values for GGG are 1.0, 3.9, and 14.4 J kg^{-1} K^{-1}, respectively, which are remarkably smaller, and the data are consistent with the results of Brodale et al. [15]. The profiles of the -ΔS_m−T curves are very consistent with their magnetic natures. As LiTbF$_4$ is FM in nature, its -ΔS_m−T curve peaked at a T_C value of 2.85 K. LiHoF$_4$ exhibited a T_C value of approximately 1.53 K, which is just beyond the current measurement interval, but there is a saturation tendency as the temperature is lowered to 1.8 K. Regarding the other compounds, which either have much lower magnetic ordering temperatures (LiDyF$_4$, LiErF$_4$, and LiYbF$_4$) or are PM in nature (LiGdF$_4$), their -ΔS_m−T curves exhibited a monotonous increasing tendency. -ΔS_m of LiTmF$_4$ was marginal due to its Van-Vleck paramagnetism. Regarding all the LiREF$_4$ crystals, the magnetization and demagnetization curves greatly overlapped, which indicates the excellent magnetic reversibility of the MCE (Supplementary Fig. 9).

Just as the magnetic isotherms indicate remarkable magnetocrystalline anisotropy, as shown in Supplementary

Figs. 1–7, -ΔS_m greatly differs between the easy and hard axes. Choosing LiTbF$_4$ as an example, the maximum -ΔS_m values along the magnetic hard axis were 1.2, 4, and 10.7 J kg^{-1} K^{-1} under 5, 10, and 20 kOe, respectively, which are much smaller than the values of 10.1, 17.9, and 21.2 J kg^{-1}K^{-1}, respectively, along the easy axis. In addition, -ΔS_m along the hard axis of LiDyF$_4$ was negative, which might be attributed to the unique crystal electric field effects. From the temperature dependence of magnetization under the different magnetic fields (Supplementary Fig. 8), the magnetization was suppressed under magnetic fields below 5 K, and the minimum value slightly shifted to higher temperatures. In terms of the magnetic Maxwell relation, this negative -ΔS_m value is understandable.

Rotating MCEs of LiREF$_4$

As reflected by the observed magnetizations and conventional MCEs above, the LiREF$_4$ single crystals exhibited very high magnetocrystalline anisotropy. Consequently, large rotating MCEs are highly anticipated. Under the conventional magnetic refrigeration

scenario, magnetization and demagnetization processes are realized by moving the magnetocaloric materials in and out of the magnetic field zone, respectively. However, effective magnetic fields can be tuned by rotating the magnetocaloric single crystals (the rotating MCE). The magnetization process is actualized when the magnetic easy axis of the single crystals is oriented along the direction of the external magnetic fields, after which the single crystals are rotated by 90 degrees to achieve demagnetization. Thus, the entropy changes of the rotating MCE, ΔS_r, can be defined as the difference in ΔS_m between the magnetic easy and hard axes. This system indeed exhibits considerable rotating MCEs, as shown by the temperature dependency of ΔS_r under 5, 10, and 20 kOe in Fig. 3. Except for LiTmF$_4$ (not shown here), the maxima of ΔS_r for the other fluorides are all higher than $10 \, \mathrm{J \, kg^{-1} \, K^{-1}}$ under 20 kOe. Since the magnetic entropy change of LiREF$_4$ along the hard axis is very small, its rotating magnetic entropy change is almost the same as that along the easy axis. The largest value is obtained for LiHoF$_4$, at $22.6 \, \mathrm{J \, kg^{-1} \, K^{-1}}$. In fact, the maximum ΔS_r value exceeds $21.1 \, \mathrm{J \, kg^{-1} \, K^{-1}}$ even under 10 kOe for LiHoF$_4$.

ΔT_{ad} of LiREF$_4$

In addition to the isothermal magnetic entropy change, the adiabatic temperature change (ΔT_{ad}) is another critical parameter characterizing magnetocaloric materials, which is defined as the temperature change of a magnetocaloric material in response to varying magnetic fields under adiabatic conditions. ΔT_{ad} can be adopted to evaluate the real performance in magnetic refrigeration applications more easily. A larger ΔT_{ad} value underlies a sharper temperature gradient between the magnetic refrigeration working material and thermal loading, which facilitates heat exchange.
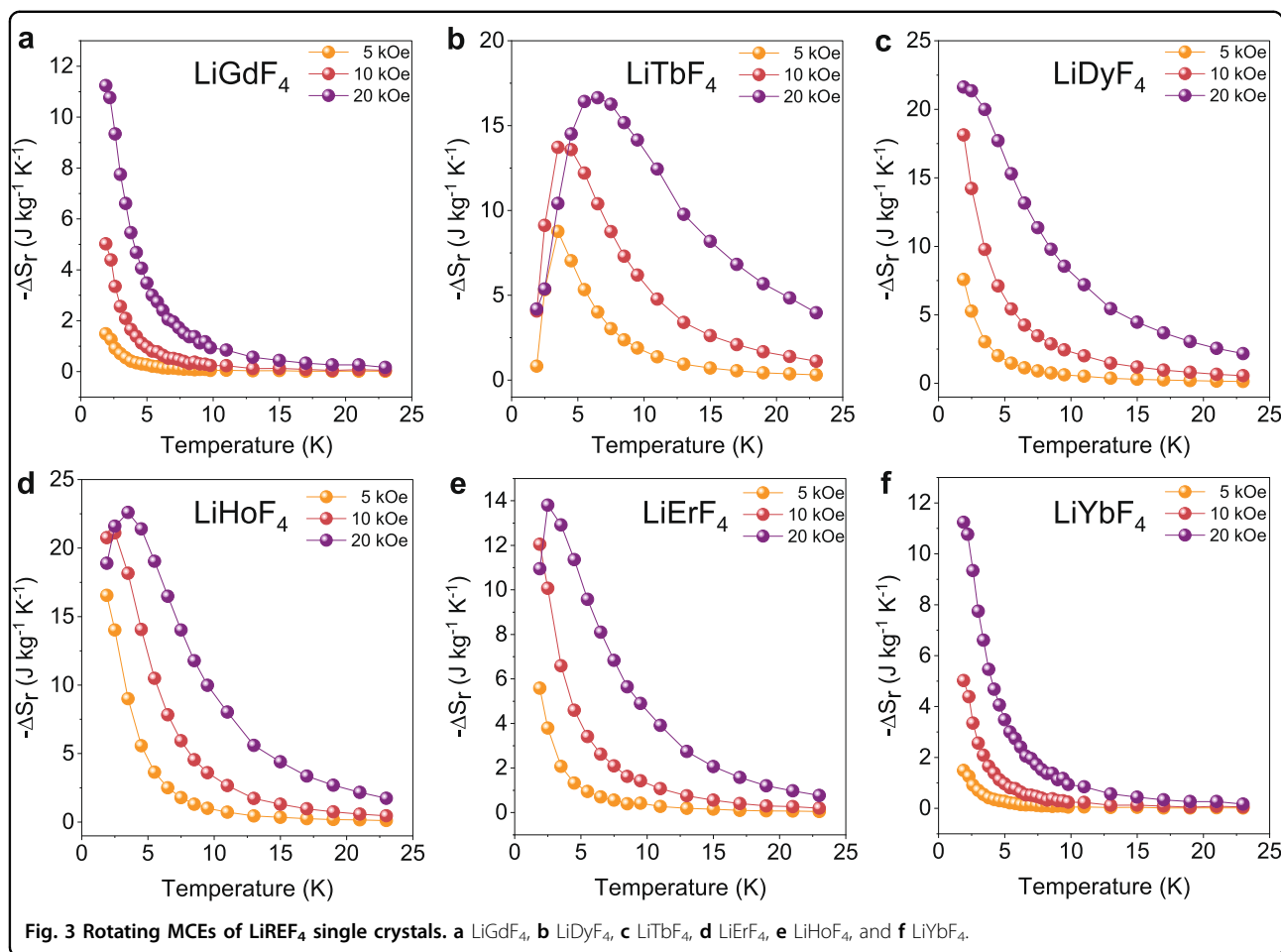
The direct ΔT_{ad} value can be measured using pulsed magnetic fields under nearly adiabatic conditions, which was achieved in magnetocaloric Gd and GGG[35,36]. In regard to FM LiTbF$_4$ and LiHoF$_4$ as well as AFM LiDyF$_4$ single crystals, pulsed magnetic fields were applied along their easy axes, as shown in Fig. 4a−c. At a given initial base temperature (T_b), the temperature of the sample (T_s) was recorded as the pulsed magnetic fields increased to 250 kOe and decreased to 0. The direct ΔT_{ad} value can be defined as the difference between T_s and T_b. Due to the short pulse structure and thus nearly ideal thermal insulation, this temperature increase is quite close to the theoretical ΔT_{ad} value. The ΔT_{ad} values at magnetization and demagnetization nearly coincide, which indicates the cycling ability. The largest ΔT_{ad} value of LiTbF$_4$ was obtained at 4.2 K, which is as high as 30 K, consistent with a previous study[37]. It is reasonable that LiTbF$_4$ is FM in nature below 2.85 K, and the largest magnetic fluctuations

are expected at a temperature slightly higher than T_C. The FM nature was also manifested in the saturation tendency of ΔT_{ad} under higher magnetic fields. FM LiHoF$_4$ also exhibited the same properties. As a benchmark, AFM LiDyF$_4$ was also considered under similar conditions. Notably, the profiles of ΔT_{ad} did not show saturation behavior, conforming with its AFM nature. In Fig. 4d, ΔT_{ad} of LiHoF$_4$ in the region below 5 kOe is highlighted. At the base temperature of 1.6 K, the highest value was obtained, reaching as high as 2.38 K. In other words, adiabatic removal of the magnetic field of 5 kOe at approximately 4 K leads to cooling to 1.6 K.

Discussion

LiREF$_4$ has shown great potential as a magnetocaloric material since Numazawa et al. investigated the magnetocaloric effects of polycrystalline LiGdF$_4$ in 2006[23]. Very recently, polycrystalline LiGdF$_4$, LiHoF$_4$, and LiErF$_4$ have also been reported with entropy changes of 44, 25.9, and $17.5 \, \mathrm{J \, kg^{-1} \, K^{-1}}$, respectively, under 20 kOe[21,23,38]. Due to the high magnetocrystalline anisotropy, the polycrystalline samples exhibited a limited performance under a small magnetic field. Here, by using a single crystal, the magnetocaloric performance under small magnetic fields was significantly improved. Under magnetic fields of 5 kOe, LiHoF$_4$ yielded the largest -ΔS_m value among all fluorides. As listed in Table 1, LiHoF$_4$ holds the record of -ΔS_m among these known magnetocaloric compounds.

The encouraging results here for LiREF$_4$ single crystals open an emergent route to compact magnetic refrigerators around liquid-helium temperature intervals or even lower. First, -ΔS_m and ΔT_{ad}, as two critical factors for magnetic refrigeration, are significantly larger than those of the prototype GGG. This feature ensures that fewer working materials are necessary for a given refrigeration loading, which reduces the volume of the whole refrigerator. Second, under a small magnetic field, such as 10 kOe or even 5 kOe, which can be easily generated by a permanent magnet, the magnetocaloric performance of these single crystals is almost saturated. In contrast, current magnetic refrigerators can only be operated under large magnetic fields, and superconducting magnets are mandatory. For example, Kwon et al. designed a refrigerator consisting of a sorption cooler and an adiabatic demagnetization refrigerator, in which the magnetic working medium was GGG under a magnetic field of 40 kOe[17]. It has been recognized that the volume or weight of the superconducting magnets accounts for approximately one-third of the whole system[39]. Thus, the replacement of a superconducting magnet with a permanent magnet is anticipated to greatly reduce the cost and volume of the whole system. Third, the significant reduction in the working magnetic fields greatly simplifies the magnetic shielding system necessary for high-

Fig. 3 Rotating MCEs of LiREF$_4$ single crystals. a LiGdF$_4$, **b** LiDyF$_4$, **c** LiTbF$_4$, **d** LiErF$_4$, **e** LiHoF$_4$, and **f** LiYbF$_4$.

precision detection. Without a complicated magnetic shielding system, the volume of the system can be further reduced. Fourth, the superior rotating MCEs discovered in LiREF$_4$ single crystals provide a chance to achieve much smaller devices than the conventional reciprocating configuration, as schematically shown in Supplementary Fig. 10. Finally, the magnetic ordering temperatures of this family cover a very wide temperature region, where T_N of LiYbF$_4$ is as low as 0.128 K, enabling ultralow-temperature applications.
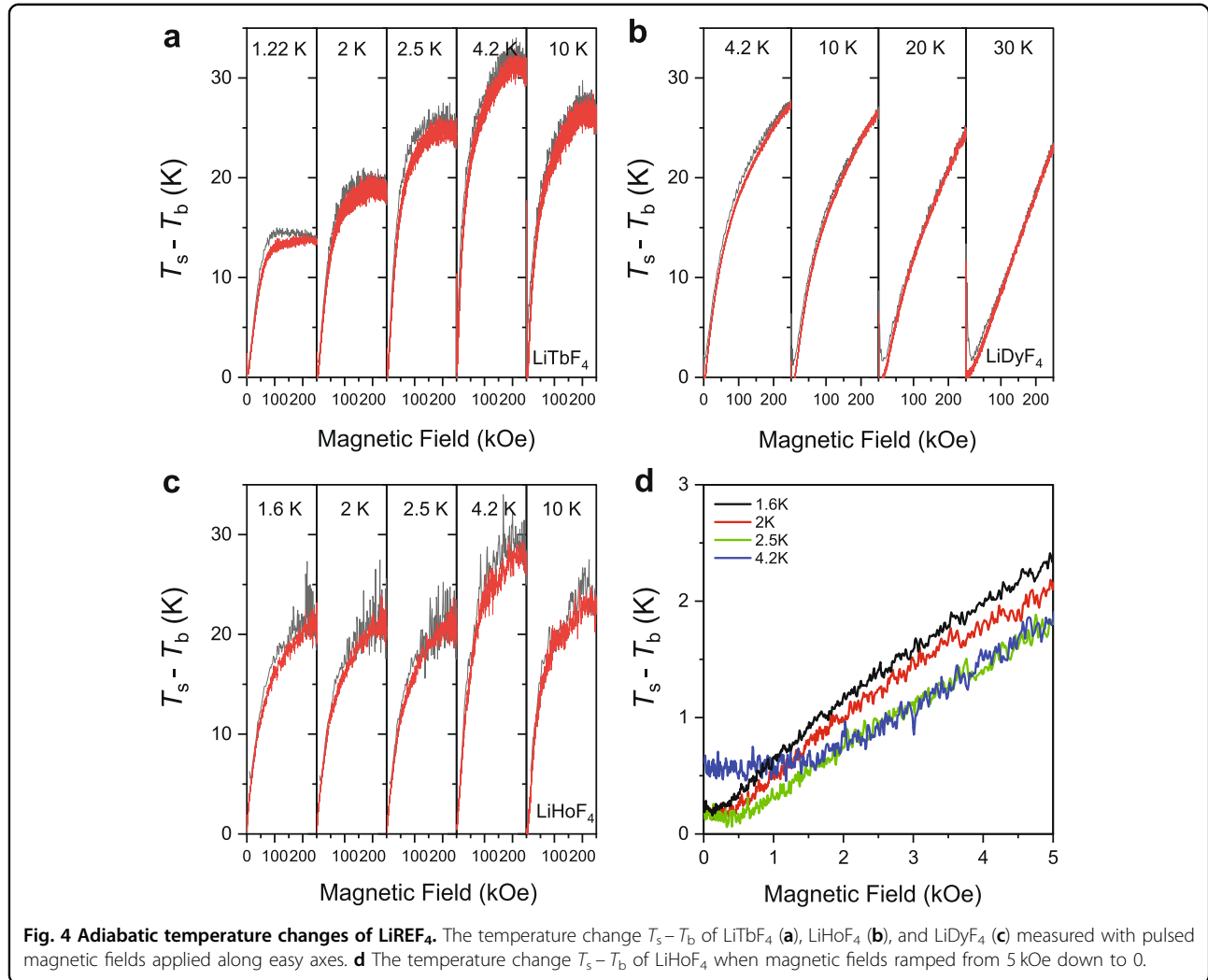
In summary, we systematically investigated the magnetocaloric properties of single crystals of the LiREF$_4$ family, including LiGdF$_4$, LiTbF$_4$, LiHoF$_4$, LiDyF$_4$, LiErF$_4$, LiYbF$_4$, and LiTmF$_4$. Their magnetic entropy changes were determined based on magnetization data, while the direct adiabatic temperature changes were obtained using pulsed magnetic fields. The entropy changes were significantly larger than those of the reference GGG single crystals. The very high magnetocrystalline anisotropy also resulted in notable rotating MCEs. In LiHoF$_4$, specifically, the magnetic entropy change and the direct adiabatic temperature change reached 16.73 J kg^{-1} K^{-1} and 2.38 K under 5 kOe,

respectively. This superior magnetocaloric performance renders this system promising in terms of replacing GGG as a next-generation working material for compact magnetic refrigeration around liquid-helium temperatures.

Methods

Sample preparation and structural characterizations

LiREF$_4$ single crystals were grown by the Czochralski technique using a resistive or an RF-heating furnace. Powders (<99.99%) were loaded into a Pt crucible, where they were subjected to a fluorination process. Then, crystal growth was achieved in a high-purity CF$_4$ (99.99%) atmosphere to effectively eliminate oxygen traces from the chamber. Single crystals were grown using *a*-oriented LiYF$_4$ seeds. The details on crystal growth have been published elsewhere[40]. The single crystals were structurally characterized using powder X-ray diffraction (Supplementary Fig. 11) as well as the Laue back-reflection method (Supplementary Fig. 12). The alignments of the single crystals for magnetic measurements were also determined using the Laue back-reflection method. GGG single crystals were

Fig. 4 Adiabatic temperature changes of LiREF₄. The temperature change $T_s - T_b$ of LiTbF$_4$ (**a**), LiHoF$_4$ (**b**), and LiDyF$_4$ (**c**) measured with pulsed magnetic fields applied along easy axes. **d** The temperature change $T_s - T_b$ of LiHoF$_4$ when magnetic fields ramped from 5 kOe down to 0.

purchased from Hefei Kejing Materials Technology Co., Ltd.

Magnetic experiments

The magnetic properties of the LiREF$_4$ single-crystal samples as well as the reference GGG single crystals were measured using a superconductor quantum interference device magnetometer (MPMS-XL, Quantum Design). Magnetic fields were applied along the magnetic easy and hard axes. The magnetic entropy changes ΔS_m were calculated based on magnetic isotherms according to the Maxwell relationship[41]:

$$\triangle S_m(T,H) = \int_0^H \left(\frac{\partial M}{\partial T}\right)_H dH = \frac{1}{T_1 - T_2}\left[\int_0^H M(T_1,H)dH - \int_0^H M(T_2,H)dH\right] \tag{1}$$

Regarding the rotating MCE, the magnetic entropy change was defined as the difference in ΔS_m when the magnetic fields are oriented along the hard and easy axes,

as follows:

$$\triangle S_r = \triangle S_{H\|\text{easy}} - \triangle S_{H\|\text{hard}} \tag{2}$$

In this rotating process, the effective magnetic fields were increased, so $\triangle S_r < 0$.

Direct measurement of the adiabatic temperature change

ΔT_{ad} of the LiREF$_4$ single crystals were measured at the Wuhan National High Magnetic Field Center, Huazhong University of Science and Technology. Pulsed high fields up to 250 kOe were generated by a long-pulse magnet with a duration of 80 ms, and the exact temperature was detected by a thin film RuO$_2$ thermometer on the surface of the sample. At various base temperatures, T_s versus H curves of the LiREF$_4$ single crystals were obtained under pulsed magnetic fields applied along the easy axis. ΔT_{ad} was calculated from T_s–H data by subtracting the corresponding initial base temperature[35,36,41].

Table 1 Comparison of magnetic entropy change (-ΔS_m) of leading magnetocaloric materials under a magnetic field changing from 0 to 5 kOe.

Materials	-ΔS_m (J·kg^{-1}K^{-1})
GGG	1.08[a]
GGG	1.0
Gd(OH)$_3$	2.1[b]
GdPO$_4$ nanorods	6.6[c]
GdF$_3$ polycrystals	10.7[d]
Ho$_{12}$Co$_7$	1.8[e]
LiGdF$_4$ single crystals	6.6
LiHoF$_4$ polycrystals	8.5[f]
LiHoF$_4$ single crystals	16.7
LiTbF$_4$ single crystals	10.1
LiDyF$_4$ single crystals	7.8
LiErF$_4$ single crystals	6.7
LiTmF$_4$ single crystals	0.04
LiYbF$_4$ single crystals	1.7

[a]Ref. [13–15].
[b]Ref. [18].
[c]Ref. [19].
[d]Ref. [20].
[e]Ref. [22].
[f]Ref. [21].
Others obtained in this work.

Author details
^{1}School of Materials Science and Engineering, University of Science and Technology of China, 72 Wenhua Road, 110016 Shenyang, Liaoning, China. ^{2}Shenyang National Laboratory for Materials Science, Institute of Metal Research, Chinese Academy of Sciences, 72 Wenhua Road, 110016 Shenyang, Liaoning, China. ^{3}National Institute for Materials Science, 1-1 Namiki, Tsukuba, Ibaraki 305-0044, Japan. ^{4}Wuhan National High Magnetic Field Center and School of Physics, Huazhong University of Science and Technology, 1037 Luoyu Road, 430074 Wuhan, Hubei, China. ^{5}Key Laboratory of Artificial Structures and Quantum Control, School of Physics and Astronomy, Shanghai Jiao Tong University, 200240 Shanghai, China

Author contributions
B.L. proposed the project. D.Y., E.G.V., and K.S. synthesized the single crystal sample. C.D. and J.W. performed the adiabatic temperature change experiments. P.L., J.Q., X.Z., Z.Z., G.L., J.M., and B.L. performed the magnetic measurements. P.L. contributed to the data analysis. P.L. and B.L. wrote the manuscript with input from all other authors.

Data availability
The data that support the findings of this study are available from the corresponding author upon request.

Conflict of interest
The authors declare no competing interests.

Publisher's note
Springer Nature remains neutral with regard to jurisdictional claims in published maps and institutional affiliations.

Supplementary information The online version contains supplementary material available at https://doi.org/10.1038/s41427-023-00488-7.

References
1. Debye, P. Einige bemerkungen zur magnetisierung bei tiefer temperatur. *Ann. Phys.* **386**, 1154–1160 (1926).
2. Giauque, W. F. A thermodynamic treatment of certain magnetic effects. A proposed method of producing temperatures considerably below 1° absolute. *J. Am. Chem. Soc.* **49**, 1864–1870 (1927).
3. Dincer, I. *Refrigeration Systems and Applications* (John Wiley & Sons, 2017).
4. Chandra, A. R. & Arora, R. C. *Refrigeration and Air Conditioning* (PHI Learning Pvt. Ltd., 2012)
5. Gutfleisch, O. et al. Magnetic materials and devices for the 21st century: stronger, lighter, and more energy efficient. *Adv. Mater.* **23**, 821–842 (2011).
6. Kittel, P. Temperature stabilized adiabatic demagnetization for space applications. *Cryogenics* **20**, 599–601 (1980).
7. Kittel, P. Magnetic refrigeration in space-Practical considerations. *J. Energ.* **4**, 266–272 (1980).
8. Kittel, P. Refrigeration below 1 K in space. *Phys. B* **108**, 1115–1117 (1981).
9. Britt, R. D. & Richards, P. L. An adiabatic demagnetization refrigerator for infrared bolometers. *Int. J. Infrared Millim. Waves* **2**, 1083–1096 (1981).
10. Kittel, P. Ultimate temperature stability of a magnetic refrigerator. *Cryogenics* **23**, 477–478 (1983).
11. Childs, A. M., Farhi, E. & Preskill, J. Robustness of adiabatic quantum computation. *Phys. Rev. A* **65**, 012322 (2001).
12. Gaita-Ariño, A., Luis, F., Hill, S. & Coronado, E. Molecular spins for quantum computation. *Nat. Chem.* **11**, 301–309 (2019).
13. Fisher, R. A., Brodale, G. E., Hornung, E. W. & Giauque, W. F. Magnetothermodynamics of gadolinium gallium garnet. I. Heat capacity, entropy, magnetic moment from 0.5 to 4.2 K, with fields to 90 kG along the [100] axis. *J. Chem. Phys.* **59**, 4652–4663 (1973).
14. Hornung, E. W., Fisher, R. A., Brodale, G. E. & Giauque, W. F. Magnetothermodynamics of gadolinium gallium garnet. II. Heat capacity, entropy, magnetic moment from 0.5 to 4.2 K, with fields to 90 kG, along the [111] axis. *J. Chem. Phys.* **61**, 282–291 (1974).
15. Brodale, G. E., Hornung, E. W., Fisher, R. A. & Giauque, W. F. Magnetothermodynamics of gadolinium gallium garnet. III. Heat capacity, entropy, magnetic moment from 0.5 to 4.2° K with fields to 90 kG along the [110] axis. *J. Chem. Phys.* **62**, 4041–4049 (1975).
16. Jin, H. et al. Development of adiabatic demagnetization refrigerator for future astronomy missions. *Mater. Sci. Eng.* **1240**, 012027 (2022).
17. Kwon, D., Bae, J. & Jeong, S. Development of the integrated sorption cooler for an adiabatic demagnetization refrigerator (ADR). *Cryogenics* **122**, 103421 (2022).
18. Yang, Y., Zhang, Q. C., Pan, Y. Y., Long, L. S. & Zheng, L. S. Magnetocaloric effect and thermal conductivity of Gd (OH)$_3$ and Gd$_2$O (OH)$_4$(H$_2$O)$_2$. *Chem. Commun.* **51**, 7317–7320 (2015).
19. Yu, Y. Y., Petrov, D. N., Park, K. C., Huy, B. T. & Long, P. T. Magnetic and cryogenic magnetocaloric properties of GdPO$_4$ nanorods. *J. Magn. Magn. Mater.* **519**, 167452 (2021).
20. Chen, Y. C. et al. A brilliant cryogenic magnetic coolant: magnetic and magnetocaloric study of ferromagnetically coupled GdF$_3$. *J. Mater. Chem. C.* **3**, 12206–12211 (2015).
21. Xie, H. et al. Giant and reversible low field magnetocaloric effect in LiHoF$_4$ compound. *Dalton Trans.* **50**, 17697–17702 (2021).
22. Zheng, X. Q. et al. Giant magnetocaloric effect in Ho$_{12}$Co$_7$ compound. *Appl. Phys. Lett.* **102**, 022421 (2013).

23. Numazawa, T., Kamiya, K., Shirron, P., DiPirro, M. & Matsumoto, K. Magneto-caloric effect of polycrystal GdLiF$_4$ for adiabatic magnetic refrigeration. *AIP Conf. Proc.* **850**, 1579–1580 (2006).

24. Holmes, L. M., Johansson, T. & Guggenheim, H. J. Ferromagnetism in LiTbF$_4$. *Solid State Commun.* **12**, 993–997 (1973).

25. Romanova, I. V., Malkin, B. Z., Mukhamedshin, I. R., Suzuki, H. & Tagirov, M. S. Magnetic properties of the Ising dipole ferromagnet LiTbF$_4$. *Phys. Solid State* **44**, 1544–1549 (2002).

26. Als-Nielsen, J., Holmes, L. M., Larsen, F. K. & Guggenheim, H. J. Spontaneous magnetization in the dipolar Ising ferromagnet LiTbF $_4$. *Phys. Rev. B* **12**, 191 (1975).

27. Romanova, I. V. et al. Magnetic and magnetoelastic properties of LiDyF$_4$ single crystals. *J. Phys. Conf. Ser.* **478**, 012026 (2013).

28. Mennenga, G., de Jongh, L. J. & Huiskamp, W. J. Field dependent specific heat study of the dipolar Ising ferromagnet LiHoF$_4$. *J. Magn. Magn. Mater.* **44**, 59–76 (1984).

29. Beauvillain, P., Renard, J. P., Laursen, I. & Walker, P. J. Critical behavior of the magnetic susceptibility of the uniaxial ferromagnet LiHoF$_4$. *Phys. Rev. B* **18**, 3360 (1978).

30. Kraemer, C. et al. Dipolar antiferromagnetism and quantum criticality in LiErF$_4$. *Science* **336**, 1416–1419 (2012).

31. Abubakirov, D. I., Matsumoto, K., Suzuki, H. & Tagirov, M. S. Anisotropic magnetization of the Van Vleck paramagnet LiTmF$_4$ at low temperatures and high magnetic fields. *J. Phys. Condens. Mat.* **20**, 395223 (2008).

32. Babkevich, P. et al. Dimensional reduction in quantum dipolar antiferromagnets. *Phys. Rev. Lett.* **116**, 197202 (2016).

33. Mennenga, G., de Jongh, L. J., Huiskamp, W. J. & Laursen, I. A comparative study of the magnetic ordering specific heats of four S=1/2 dipolar magnets: LiRF$_4$ (R=Er, Dy, Ho, Tb). *J. Magn. Magn. Mater.* **44**, 48–58 (1984).

34. Babkevich, P. et al. Neutron spectroscopic study of crystal-field excitations and the effect of the crystal field on dipolar magnetism in LiRF$_4$ (R= Gd, Ho, Er, Tm, and Yb). *Phys. Rev. B* **92**, 144422 (2015).

35. Kihara, T., Kohama, Y., Hashimoto, Y., Katsumoto, S. & Tokunaga, M. Adiabatic measurements of magneto-caloric effects in pulsed high magnetic fields up to 55 T. *Rev. Sci. Instrum.* **84**, 074901 (2013).

36. Miyake, A. et al. Capacitive detection of magnetostriction, dielectric constant, and magneto-caloric effects in pulsed magnetic fields. *Rev. Sci. Instrum.* **91**, 105103 (2020).

37. Kazei, Z. A., Snegirev, V. V., Broto, J. M., Abdulsabirov, R. Y. & Korableva, S. L. Induced quadrupole effects near a crossover in a tetragonal TbLiF4 sheelite in a strong magnetic field up to 50 T. *J. Exp. Theor. Phys.* **115**, 1029–1041 (2012).

38. Mo, Z. et al. Giant low-field cryogenic magnetocaloric effect in polycrystalline LiErF4 Compound. *Chin. Phys. B* **32**, 027503 (2022).

39. Martinis J. M. *Mechanical Support for a Two Pill Adiabatic Demagnetization Refrigerator.* United States Patent 5934077 (1999).

40. Vasyliev, V., Villora, E. G., Nakamura, M., Sugahara, Y. & Shimamura, K. UV-visible Faraday rotators based on rare-earth fluoride single crystals: LiREF$_4$ (RE = Tb, Dy, Ho, Er and Yb), PrF$_3$ and CeF$_3$. *Opt. Express* **20**, 14460 (2012).

41. Pecharsky, V. K. & Gschneidner, K. A. Jr Magnetocaloric effect from indirect measurements: Magnetization and heat capacity. *J. Appl. Phys.* **86**, 565–575 (1999).